

Nonstationary ground motion spatial correlations in CyberShake simulations, and implications for regional risk analysis

PI: JACK W. BAKER GRADUATE RESEARCHER: YILIN CHEN
Department of Civil and Environmental Engineering
Stanford University

July 19, 2018

Abstract

Spatial variations in strong ground motion have a significant impact on performance of distributed infrastructure in earthquakes. These variations are also of great importance to insurance companies that have earthquake insurance policies for many buildings in a region. Currently, these spatial variations are measured using ground motion data from densely recorded earthquakes. While useful, this measurement process requires strong assumptions about stationarity and anisotropy of correlations.

This project has performed analogous spatial variations calculations on simulations from the CyberShake platform. The richness of that simulation set has allowed significant relaxation of these assumptions, and offered insights regarding the role of source and path heterogeneity on the spatial correlation of ground motion amplitudes. This work indicates an opportunity for a new dimension of ground motion simulation validation, as the estimated correlations can be compared to results from past earthquakes. Finally, this work helps make the case for the value of using physical simulations when evaluating risk to distributed infrastructure systems.

1 Introduction

When an earthquake causes shaking in a region, the amplitude of shaking (measured, for example, using spectral acceleration at a given period) varies spatially. Some of that variation is predicable, via attenuation, near-surface site effects, basin effects, and other phenomena. Empirical ground motion prediction models capture those effects, but there is significant remaining variation in ground motion amplitudes not captured by those models. This remaining variation in ground motion prediction “residuals” is significant, and shows spatial correlation at scales of 10’s of km in separation distance. This spatial correlation is expected, due to commonalities in crustal velocity structure and wave propagation paths, and has been shown by a number of researchers to be important when assessing risk to spatially distributed infrastructure or portfolios of properties.

2 Methodology

According to the ground-motion model,

$$\ln SA_{ik} = \overline{\ln SA_{ik}} + \sigma_{ik} \varepsilon_{ik} \quad (1)$$

where SA_{ik} is the spectral acceleration geometric mean at site i under earthquake k ; $\overline{\ln SA_{ik}}$ is the natural logarithmic mean of spectral acceleration intensity; $\sigma_{ik} \varepsilon_{ik}$ represents the residual at site j with standard deviation σ_{ik} , and ε_{ik} is the standard normal random variable.

The semivariogram is a popular geostatistical tool to measure the dissimilarity of spatially distributed data. It represents half the squared difference between the components of data pair of location \mathbf{u}, \mathbf{u}' :

$$\gamma(\mathbf{u}, \mathbf{u}') = \frac{1}{2} \mathbb{E}[(z(\mathbf{u}) - z(\mathbf{u}'))^2] \quad (2)$$

which can be empirically estimated with:

$$\gamma(\mathbf{u}, \mathbf{u}') = \frac{1}{2N(\mathbf{u}, \mathbf{u}')} \sum_{\alpha=1}^{N(\mathbf{u}, \mathbf{u}')} [z(\mathbf{u}_\alpha) - z(\mathbf{u}'_\alpha)]^2 \quad (3)$$

Since one often does not possess several records of ground motion at a given pair of sites, the assumptions of stationarity and isotropy have to be made in order to evaluate Equation 2. Under these assumptions, semivariogram can be specified by the separation distance h only:

$$\gamma(h) = \frac{1}{2N(h)} \sum_{\alpha=1}^{N(h)} [z(\mathbf{u}_\alpha) - z(\mathbf{u}_\alpha + h)]^2 \quad (4)$$

Furthermore, the covariance between $z(\mathbf{u})$ and $z(\mathbf{u} + h)$ is defined as:

$$C(h) = \mathbb{E}[(z(\mathbf{u} + h) - \mathbb{E}[z(\mathbf{u} + h)])(z(\mathbf{u}) - \mathbb{E}[z(\mathbf{u})])] \quad (5)$$

We can further show that the correlation coefficient for $z(\mathbf{u})$ and $z(\mathbf{u} + h)$ is:

$$\rho(h) = \frac{C(h)}{C(0)} = 1 - \frac{\gamma(h)}{C(0)} \quad (6)$$

Therefore, we can estimate the correlation coefficient at distance h by calculating its empirical semivariogram.

3 Results

Since CyberShake simulations allow us to calculate correlation coefficients between every pair of sites across the region, we can examine the impact of other factors except for separation distance.

3.1 Dependence on geological condition

In order to investigate the effect of geologic condition on spatial correlations, we pick a reference site and calculate the correlation coefficient between every other site and the reference site. Then a heat map of correlation coefficients is provided to visualize the effect of geologic condition.

As shown in Figure 1, the distribution of the correlation coefficients is similar to the empirical model. However, the basin regions (the bottom left and upper right part on the map) do show a higher correlation level than rocky regions. The phenomenon of correlation coefficient decreasing as distance increases can be explained by a reduction in common source and path effects, since the closer the two sites are, the more likely their shaking is influenced by the same factors. In the meantime, the path effect might contribute to the magnification of correlation in the basin region: When an earthquake wave propagates into a basin region, it will pass back and forth several times before losing its power, and thus the path effect is enhanced, which results in a higher correlation level in a basin region.

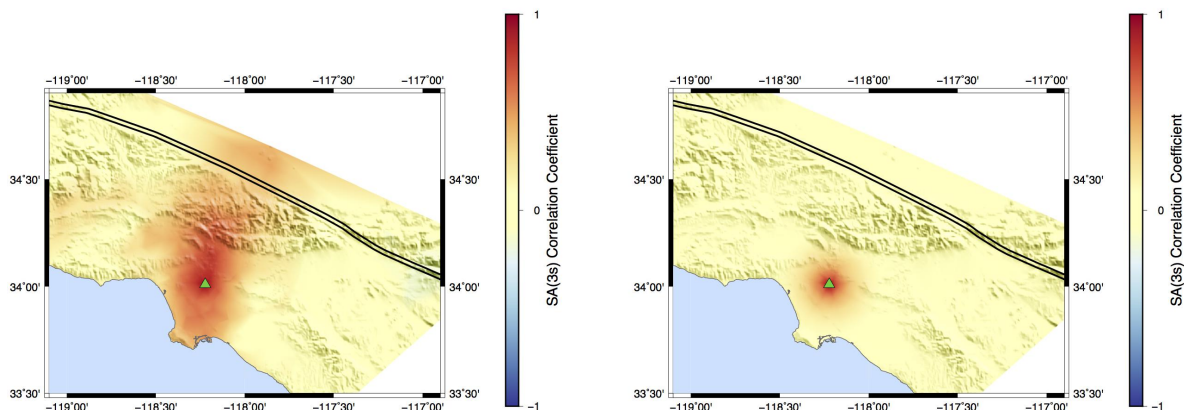


Figure 1: Heat map of correlation coefficients for spectral acceleration at $T=3s$ caused by San Andreas rupture. CyberShake Simulation (left); Empirical Model (right). A reference site is indicated by a triangle, and correlation coefficients between this site and all other sites in the region are indicated by colored shading.

3.2 Dependence on period

We follow the same calculations above but changing the period of interest to evaluate the role of period in correlation coefficients of ground motion residuals. In Figure 2, the regional distribution of correlation coefficients at periods 1s, 3s, 5s, 10s are showed respectively. It is clear that the correlation level is magnified as the period of interest increases. It is noticeable that the magnification of correlation is mainly in the basin region. For sites separated by more than 20km, period has less impact on the correlation coefficient.

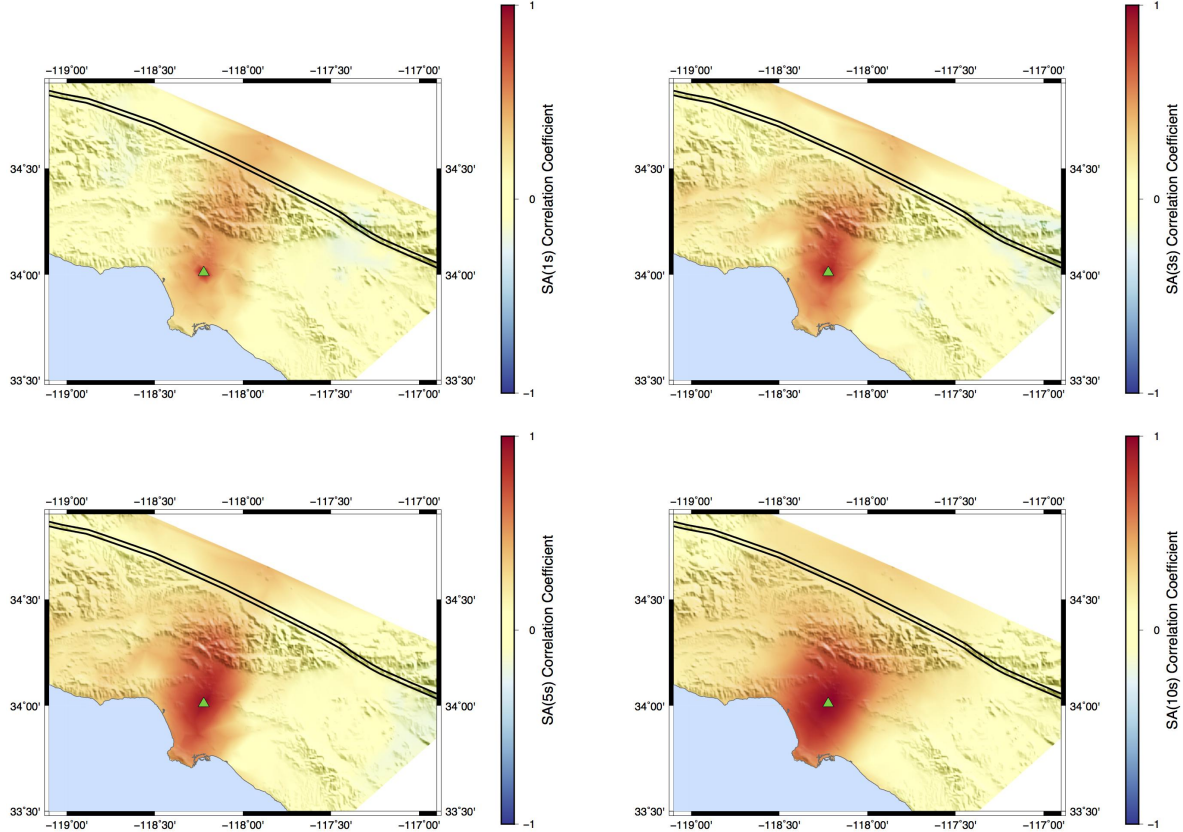


Figure 2: Heat map of correlation coefficients for spectral acceleration at $T=1s, 3s, 5s,$ and $10s$. A reference site is indicated by a triangle, and correlation coefficients between this site and all other sites in the region are indicated by colored shading.

3.3 Dependence on rupture

Figure 3 shows the heatmap of the distribution of correlation coefficients caused by two different faults, the Puente Hills rupture and San Andreas rupture. Clearly, the characteristics of the distribution are totally different. As shown in figure (b), the correlation coefficient decays as it moves away from the reference site, and it becomes almost zero when the separation distance is greater than 40km, which corresponds well to the empirical model. When it comes to the Puente Hills rupture, however, the spatial distribution shows two discrete states in the region. For the area bottom left to the rupture (LA basin), the correlation level is significantly higher than it in figure (a); For the upper right area, the correlation level is significantly lower and could even become negative.

The results showed in Figure 3 can be explained by the path effect: in the Puente Hills case, strong and concentrated waveforms propagate southward into the Los Angeles basin, which results in a high correlation in amplitudes at all sites in this area. For the northeastern region, there is barely a common path shared by adjacent sites and thus the residuals are much less correlated.

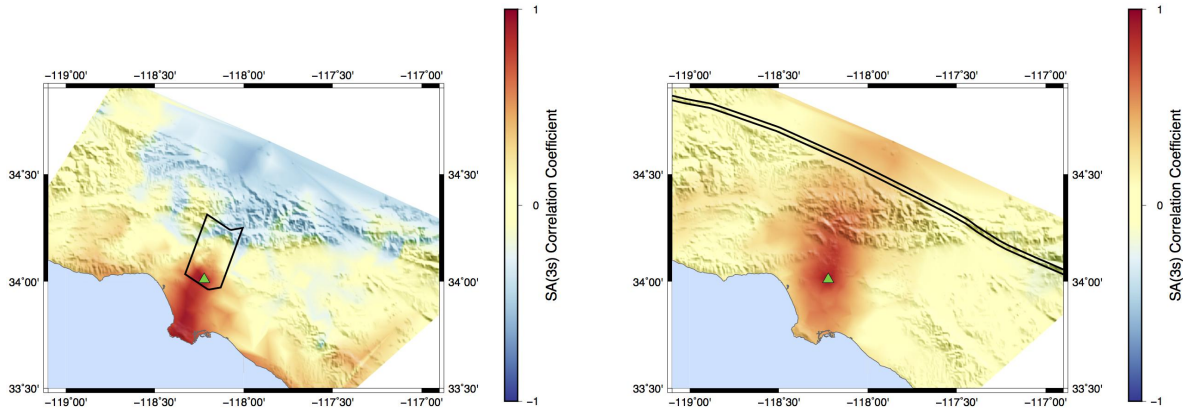


Figure 3: Heat map of correlation coefficients for spectral acceleration at $T=3s$, Puente Hills rupture (left); (b) San Andreas rupture (right). A reference site is indicated by a triangle, and correlation coefficients between this site and all other sites in the region are indicated by colored shading.

4 Conclusions

We have evaluated spatial correlation in ground motion residuals using CyberShake simulations. The results show general agreement between the distance decay of correlations relative to empirical recordings. The simulations also show strong period dependence in correlations—perhaps stronger than empirical recordings indicate. Aside from the general agreement, the CyberShake simulations show clear non-stationary spatial correlations. The figures above indicate amplified spatial correlations in the Los Angeles basin, likely due to the enhancement of shared path effects. Rupture propagation directivity also appears to have effects on spatial correlation: the correlation coefficients tend to be higher along the propagation direction than in other orientations. In down-rupture versus up-rupture directions, correlation coefficients can even be negative in the CyberShake simulations.

Anticipated follow-on work to this project will further evaluate differences between simulated and recorded motions’ spatial correlations, and will evaluate the effect of alternate statistical estimation techniques.

5 Acknowledgements

We thank Scott Callaghan for help accessing the CyberShake database. This research was supported by the Southern California Earthquake Center (Contribution No. 7963). SCEC is funded by NSF Cooperative Agreement EAR-1033462 & USGS Cooperative Agreement G12AC20038.